PROCEEDINGS OF SCIENCE

Experimental review of rare charm decays

Tengjiao Wang, for the BESIII Collaboration[a,*]

[a] *Nankai University,*
94 Weijin, Tianjian, China

E-mail: wangtj@mail.nankai.edu.cn

Standard Model is the most well tested model yet, but still it is an incomplete theory. There are fundamental physical phenomena in nature that the Standard Model does not adequately explain. Complementary to the down-type quark studies in the K and B sectors, decays containing the charm quark are a unique window to find the signal beyond the Standard Model. In this proceeding, 8 recent experimental results searching for the new physics signals through rare charm decays are reviewed.

16th International Conference on Heavy Quarks and Leptons (HQL2023)
28 November-2 December 2023
TIFR, Mumbai, Maharashtra, India

*Speaker

PoS(HQL2023)048

1. Introduction

Forbidden or highly suppressed charm decays in the Standard Model (SM) open a good window to search for the beyond SM signals, such as processes of Flavor Changing Neutral Currents (FCNC), baryon number violation (BNV), and lepton number violation (LNV). Processes with a change in quark falvor without a change in electric charge are forbidden at the lowest order in the SM of particle physics. FCNC processes are additionally suppressed by the Glashow-lliopoulos-Maiani (GIM) mechanism [1]. Complementary to the down-type quark studies in the K and B sectors, the GIM mechanism is suppressed more strongly in charm sector. In addition, as demonstrated by the stability of ordinary matter, a baryon number (B) is empirically known to be conserved to a very high degree. However, the absolute conservation of B has been questioned for many years. For example, the fact that there is an excess of baryons over anti-baryons in the Universe implies the existence of BNV processes. Therefore, various extensions of the SM with BNV processes have been proposed. Thus, a study for BNV processes also can search for the new physics signals.

The large data samples collected by the BESIII, Belle, and LHCb detectors provide a good opportunity to search for new physics signals through rare charm decays. In this proceeding, we review the recent experimental results at BESIII, Belle, and LHCb collaboration.

2. FCNC processes

2.1 $D^0 \to \pi^0 \nu\bar{\nu}$

For D FCNC decays into final states involving di-neutrinos, such as $D^0 \to \nu\nu$, long-distance contributions become insignificant and the short-distance contributions from Z penguin and box diagrams dominate, resulting in the branching fraction at the level of 10^{-15} in SM [2]. That makes D FCNC decay involving di-neutrinos a unique and clean probe to study the CP violation in the charm sector [3] and search for new physics beyond SM [4].

In 2022, BESIII present the first experimental search for the FCNC process $c \to u\nu\bar{\nu}$ through $D^0 \to \pi^0\nu\bar{\nu}$ decay with 10.6×10^6 pairs of $D^0\bar{D}^0$ mesons produced by e^+e^- collisions near threshold [5]. Figure 1 presents the $E_{\rm EMC}$ distribution in data, on which the result of an extended maximum likelihood fit is overlaid. The fit determines the signal yield $N_{\rm sig}$ to be 14 ± 30, which is consistent with zero. No obvious signal is observed and an upper limit (UL) on its decay branching fraction is set to be 2.1×10^{-4} at 90% confidence level (CL). This is the world-first experimental constraint in charmed hadron decays to a dineutrino final state.

2.2 $\Lambda_c^+ \to p\gamma'$

Models of new physics beyond the SM may have a dark sector containing an extra Abelian gauge group, $U(1)_D$, under which all the SM fields are singlets. If $U(1)_D$ remains unbroken, then there is always a linear combination of the dark and SM Abelian gauge fields which does not have renormalizable couplings to SM members and which can be identified with the massless dark photon (γ') [6, 7]. While it has no direct interactions with SM fermions, the γ' can still exert influence on the SM via higher-dimensional operators generated by loop diagrams involving particles that are charged under $U(1)_D$ and also coupled to SM fields.

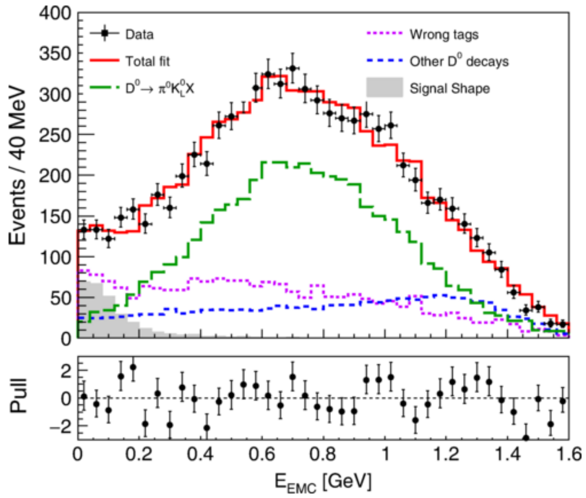

Figure 1: Fit to the E_{EMC} distribution in data. The black dots with uncertainties represent data and the red solid line shows the total fit. The background components of $D^0 \to K_L^0 \pi^0 X$ decays, wrong $\bar{D}^0$ tags and other D^0 decays are marked as green long-dashed line, purple dotted line, and blue dashed line, respectively. The gray filled area shows the signal shape, normalized to 20 times the central value of the fit result for visibility. The bottom panel shows the fit residuals.

With a sample of 4.5 fb^{-1} collected at center-of-mass energies between 4.600 and 4.699 GeV with the BESIII detector, the first investigation for a massless dark photon in $\Lambda_c^+ \to p\gamma'$ decay is carried out [8]. The distribution of $M^2_{\mathrm{rec}(\bar{\Lambda}_c^- p)}$ in the signal region is shown in Fig. (b) 2. No significant signal is observed with respect to the expected background. The UL on the branching fraction of $\Lambda_c^+ \to p\gamma'$ is measured to be $\mathcal{B}(\Lambda_c^+ \to p\gamma') < 8.0 \times 10^{-5}$ at 90% CL. It is below the sensitivity of theory prediction in Ref. [9], which predicts the branching fraction to be 1.6×10^{-5} or 9.1×10^{-6} with different inputs of form factors.

2.3 $D^0 \to \mu^+\mu^-$

The $D^0 \to \mu^+\mu^-$ decay is among the most interesting charm-hadrons decays, being fully leptonic and additionally suppressed by helicity reason. Its SM short-distance contribution is extremely suppressed, yielding a branching fraction on the order of 10^{-18} [10]. Long-distance contributions dominate through an intermediate two-photon state, and can be estimated to be $\mathcal{B}(D^0 \to \mu^+\mu^-) \simeq 2.7 \times 10^{-5}\mathcal{B}(D^0 \to \gamma\gamma)$, leading to a $D^0 \to \mu^+\mu^-$ branching fraction of at least 3×10^{-13} [10]. The $D^0 \to \mu^+\mu^-$ decay rate can be enhanced in many NP models [11]. Being one of the most sensitive FCNC processes in the charm sector, its branching fraction is used as a primary building block of different models, constraining the relevant couplings saturating the branching fraction limit.

In 2023, a search for the $D^0 \to \mu^+\mu^-$ decay [12] has been reported based on data collected by the LHCb experiment in pp collisions corresponding to 9 fb^{-1} of integrated luminosity. The data have been collected in 2011, 2012 (Run 1), and 2015-2018 (Run 2) at $\sqrt{s} = 7, 8$, and 13 TeV, respectively. The distributions projected onto $m(\mu^+\mu^-)$ and $\Delta m = m(D^{*+} - m(D^0))$ are shown in Fig. 3. No evidence for an excess of events over the expected background is observed. An UL on the

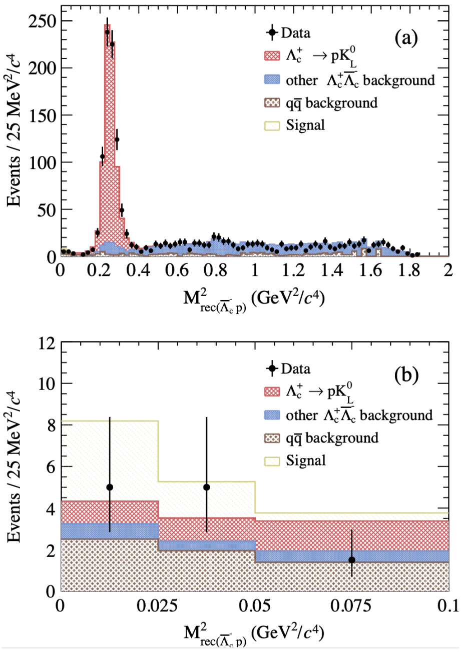

Figure 2: (a) The full spectrum of $M^2_{\mathrm{rec}(\bar{\Lambda}_c^- p)}$ of the accepted DT candidate events from the combined seven data samples. (b) The spectrum of $M^2_{\mathrm{rec}(\bar{\Lambda}_c^- p)}$ of the accepted DT candidate events from the combined data in the signal region. The black points with error bars are data; no events have been observed in the last bin. The red hatched histogram indicates pK_L^0 background. The blue hatched histogram is the $\Lambda_c^+\bar{\Lambda}_c^-$ background excluding process $\Lambda_c^+ \to pK_L^0$. The brown hatched histogram represents the $q\bar{q}$ background. The yellow hatched histogram is the $\Lambda_c^+ \to p\gamma'$ signal, which is normalized to data luminosity with the upper limit of the branching fraction.

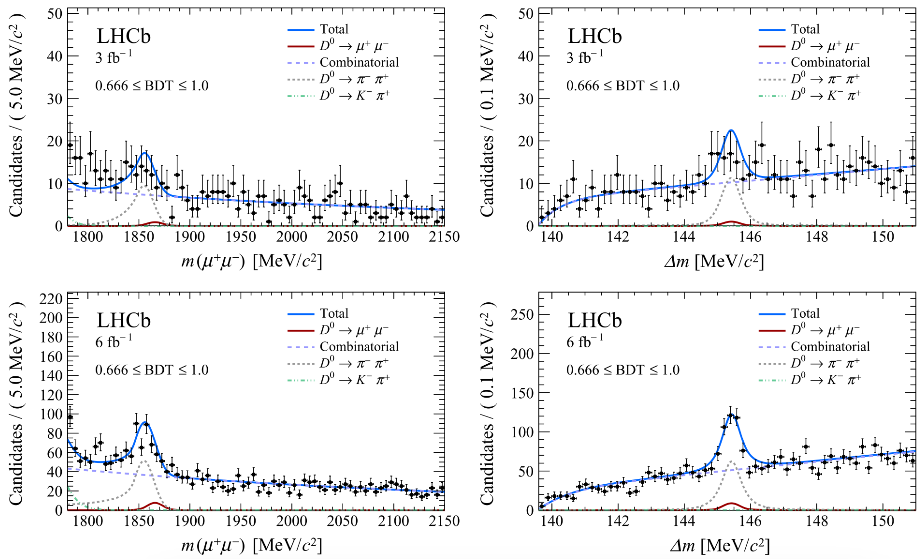

Figure 3: Distribution of (left) $m(\mu^+\mu^-)$ and (right) Δm for the $D^0 \to \mu^+\mu^-$ candidates in data from (top) Run 1 and (bottom) Run 2, for the most sensitive BDT interval. The distribution is superimposed with the fit to data. Each of the two distributions is in the signal region of the other variable; see text for details. Untagged and tagged decays are included in a single component for signal and $D^0 \to \pi^+\pi^-$ background.

PoS(HQL2023)048

branching fraction of this decay is set at $\mathcal{B}(D^0 \to \mu^+\mu^-) < 3.1 \times 10^{-9}$ at a 90% CL. This represents the world's most stringent limit, constraining models of physics beyond the standard model.

2.4 $D^*(2007)^0 \to \mu^+\mu^-$

In the same year, the very rare $D^*(2007)^0 \to \mu^+\mu^-$ decay is searched for by analysing $B^- \to \pi^+\pi^-\mu^+\mu^-$ decays. In contrast to the situation for pseudoscalar mesons, the leptonic decays of the excited vector D^{*0}, B^{*0} and B_s^{*0} states have no chiral suppression. In an effective field, these decays involve the same operators as those of the pseudoscalar mesons [13]. Therefore, if sufficient experimental precision can be obtained, leptonic decays of the vector states provide a complementary approach to constraining the associated Wilson coefficients [14]. The challenge, however, is that the vector mesons can also decay via electromagnetic and (for the D^{*0} meson) strong interactions, which have widths many orders of magnitude larger than those for the weak decays. Therefore, the branching fractions of these weak decays are strongly suppressed to levels around 10^{-11} [15, 16], unless there are large enhancements due to physics beyond the SM. For the leptonic D^{*0} decays, further suppression by the GIM mechanism reduces the SM prediction for the branching fractions to the 10^{-19} level [15, 16].

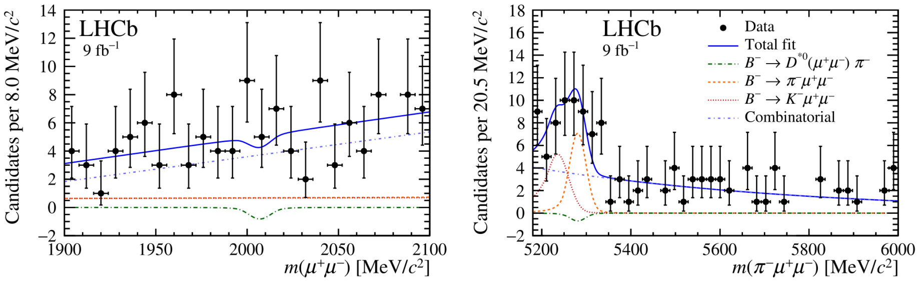

Figure 4: Reconstructed (left) $\mu^+\mu^-$ and (right) $\pi^-\mu^+\mu^-$ invariant-mass distributions for the selected $B^- \to D^{*0}(\mu^+\mu^-)\pi^-$ candidates, with results of the fit superimposed

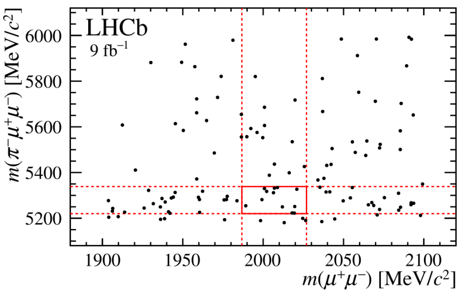

Figure 5: Two-dimensional distribution of $\mu\mu$ invariant mass versus $\pi^-\mu^+\mu^-$ invariant mass for the selected $B^- \to D^{*0}(\mu^+\mu^-)\pi^-$ candidates. The red box corresponds to a range of about $\pm 3\sigma$ around the expected signal peak position in each dimension

This analysis uses Run 1 and Run 2 collected with the LHCb detector between 2011 and 2018. Figure 4 shows the dimuon and B-candidate invariant-mass distributions of selected $B^- \to D^{*0}\pi^-$ candidates, with results of the fit superimposed. Figure 5 shows the two-dimensional distribution of selected $B^- \to D^{*0}\pi^-$ candidates. The fit favours a slightly negative yield, which is attributed to a downward fluctuation of the background in the region close to the B^- and D^{*0} meson masses. No evidence for an excess of events over background is observed and an UL is set on the branching fraction of the decay at $\mathcal{B}(D^*(2007)^0 \to \mu^+\mu^-)$ at 90% CL. This is the first limit on the branching fraction of $D^*(2007)^0 \to \mu^+\mu^-$ decays and the most stringent limit on $D^*(2007)^0$ decays to leptonic final states. The analysis is the first search for a rare charm-meson decay exploiting production via beauty decays [17].

2.5 $D^0 \to h^+h^-\mu^+\mu^-$

In 2021, LHCb experiment reported the first full angular analysis and an updated measurement of the decay-rate CP asymmetry of the $D^0 \to \pi^+\pi^-\mu^+\mu^-$ and $D^0 \to K^+K^-\mu^+\mu^-$ decays [18] by using Run1 and Run2. The short-distance contributions to the inclusive $D \to X\mu^+\mu^-$ branching fraction, where D denotes a neutral or charged D meson and X represents one or more hadrons, are predicted to be of 10^{-9} [4]. Sensitivity to FCNC processes via the measurement of branching fractions is limited due to the dominance of tree-level amplitudes involving intermediate resonances that subsequently decay into $\ell^+\ell^-$. These so-called long-distance contributions increase the SM branching fractions up to 10^{-6} [4, 19–21]. Studies of angular distributions and charge-parity (CP) asymmetries in the vicinity of intermediate resonances offer a access to observables with negligible theoretical uncertainties. These observables are sensitive to beyond SM physics through the interference between long- and short-distance amplitudes. The values of these observables are negligibly small in the SM.

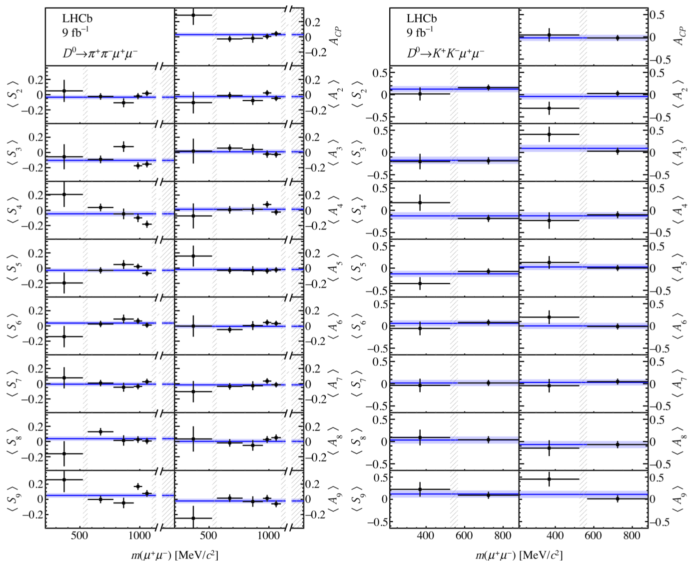

Figure 6: Measured observables for (left) $D^0 \to \pi^+\pi^-\mu^+\mu^-$ and (right) $D^0 \to K^+K^-\mu^+\mu^-$ decays in $m(\mu^+\mu^-)$ regions. No measurement is performed in the regions indicated by the vertical gray bands. The horizontal bands correspond to the measurements integrated in the dimuon mass, including candidates from all $m(\mu^+\mu^-)$ ranges. The high-mass region of $D^0 \to \pi^+\pi^-\mu^+\mu^-$ extends to 1590.5 MeV/c^2 and has been truncated on the plots for a clearer visualization of the other regions.

In this paper, the full set of CP -averaged angular observables and their CP asymmetries are measured as a function of the dimuon invariant mass. The results for $\langle S_i \rangle$, $\langle A_i \rangle$ and A_{CP}, including both statistical and systematic uncertainties added in quadrature, are reported in Fig. 6. This is the first full angular analysis of a rare charm decay ever performed. Null-test observables A_{CP}, $\langle S_{5-7}\rangle$, and $\langle A_{2-9}\rangle$ are agreement in with the SM predications with over p values of 79% (0.8%) for $D^0 \to \pi^+\pi^-\mu^+\mu^-$ ($D^0 \to K^+K^-\mu^+\mu^-$), corresponding to 0.3 (2.7) Gaussian standard deviations. The results are consistent with expectations from the standard model and with CP symmetry.

3. B/LNV processes

3.1 $D^0 \to \bar{p}e^+$ and $D^0 \to pe^-$

Several grand unified theories, supersymmetry and other SM extensions propose BNV processes of nucleons. At the level of dimension-six operators, BNV processes can happen with $\Delta(B-L) = 0$ [22]. In 2022, by analyzing 2.93 fb^{-1} of e^+e^- collision data taken at $\sqrt{s} = 3.773$ GeV, BESIII experiment searched for the SM forbidden decays $D^0 \to \bar{p}e^+$ and $D^0 \to pe^-$ with $\Delta(B-L) = 0$. Figures 7(a) and 7(b) show the distributions of $M_{\rm BC}^{\rm sig}$ vs $\Delta E^{\rm sig}$ of the candidate events for $D^0 \to \bar{p}e^+$ and $D^0 \to pe^-$ selected from the data sample, respectively. No obvious signals have been observed. The ULs on $\mathcal{B}(D^0 \to \bar{p}e^+)$ and $\mathcal{B}(D^0 \to pe^-)$ at 90% CL are set to be 1.2×10^{-6} and 2.2×10^{-6} [23], respectively. These ULs are still far above the prediction of the higher generation model.

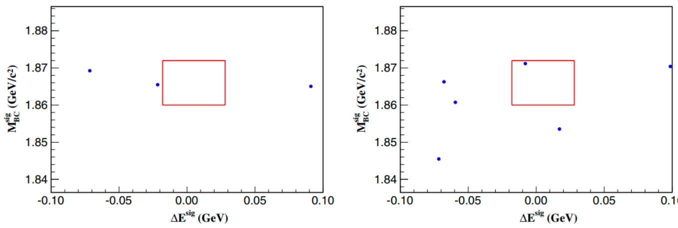

Figure 7: Distributions of $M_{\rm BC}^{\rm sig}$ vs $\Delta E^{\rm sig}$ of the candidate events for (a) $D^0 \to \bar{p}e^+$ and (b) $D^0 \to pe^-$ in data. The red rectangles denote the signal region.

3.2 $D^+ \to ne^+$

A higher-generation SUSY model predicts the branching fraction of $D^0 \to \bar{p}\ell^+ (\ell^+ = e^+, \mu^+)$ to be less than 4.0×10^{-39} [24], thus the decay $D^+ \to n\ell^+$ is also expected to be of a comparable magnitude because it differs only by the change of a spectator quark. In 2023, BESIII experiment reported the first search for the BNV process $D^{+(-)} \to \bar{n}(n)e^{+(-)}$ with $\Delta(B-L) = 0$ and $D^{+(-)} \to n(\bar{n})e^{+(-)}$ with $\Delta(B-L) = 2$, by analyzing 2.93 fb^{-1} of e^+e^- collision data taken at $\sqrt{s} = 3.773$ GeV.

An unbinned maximum-likelihood fit is performed to each $M_{n/\bar{n}}$ distribution as shown in Fig. 8. No signal is found and the ULs on branching fraction at 90% CL are determined to be $\mathcal{B}(D^+ \to \bar{n}e^+) < 1.43 \times 10^{-5}$ and $\mathcal{B}(D^+ \to ne^+) < 2.91 \times 10^{-5}$ for the processes with $\Delta(B-L) = 0$ and $\Delta(B-L) = 2$ [25], respectively.

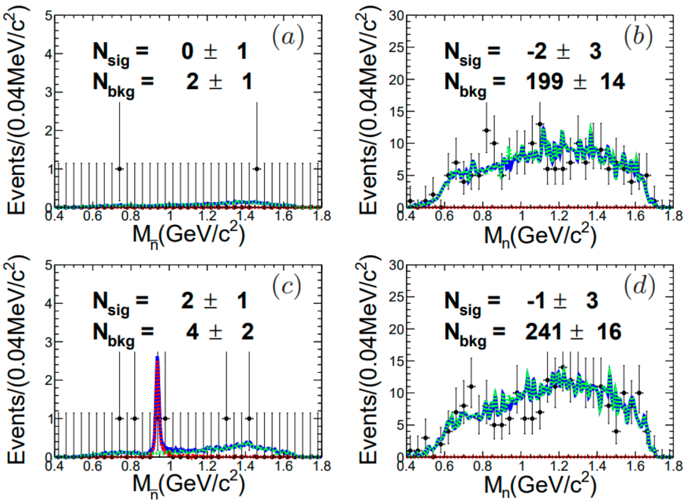

Figure 8: Fits to the $M_{n/\bar{n}}$ distributions for processes (a) $D^+ \to \bar{n}e^+$, (b) $D^- \to ne^-$, (c) $D^- \to \bar{n}e^-$ and (d) $D^+ \to ne^+$. The black dots with error bar are data. The red dotted, green dotted and blue solid lines are signal, background, and the sum of signal and background, respectively.

3.3 $D \to p\ell$

Belle also report a search for the D meson decay modes [26] $D^0 \to p\ell^-$, $\bar{D}^0 \to p\ell^-$, $D^0 \to \bar{p}\ell^+$, and $\bar{D}^0 \to \bar{p}\ell^+$, where ℓ is e or μ using data sample collected with the Belle detector at the KEKB asymmetric-energy e^+e^- collider. The data used in this analysis were collected at e^+e^- center-of-mass energies at and 60 MeV below the $\Upsilon(4S)$ resonance, and at the $\Upsilon(5S)$ resonance with integrated luminosities of 711 fb^{-1}, 89 fb^{-1}, and 121 fb^{-1}, respectively.

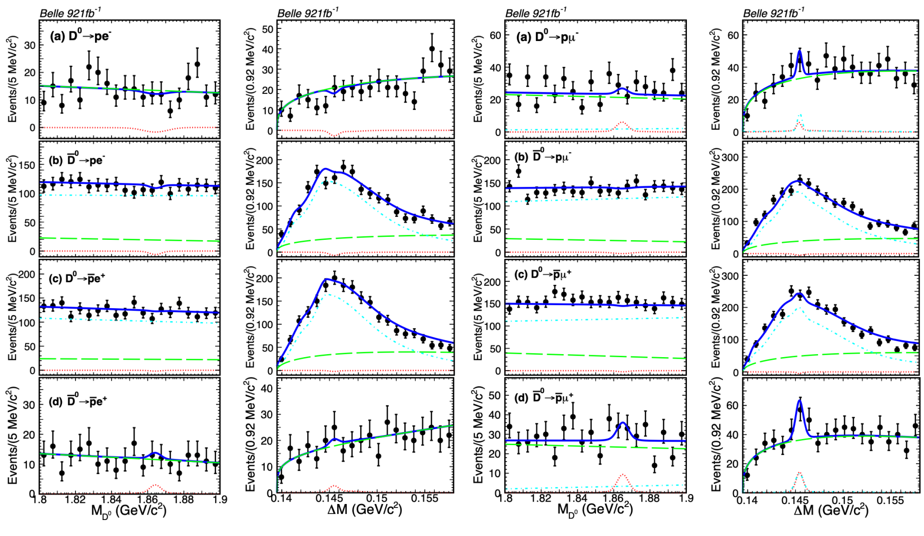

Figure 9: Fit projections for the M_{D^0} and ΔM distributions for the (a) $D^0 \to pe^-(\mu^-)$, (b) $\bar{D}^0 \to pe^-(\mu^-)$, (c) $D^0 \to \bar{p}e^+(\mu^+)$, and (d) $\bar{D}^0 \to \bar{p}e^+(\mu^+)$ decay modes. The red dotted curves show the fit function for the signal, the green dashed curves show the fit function for the combinatorial background, the cyan dashed-dotted curves show the fit function for the peaking background, and the blue solid curves show the sum of the fit functions.

The fit projections for the M_{D^0} and ΔM distributions are shown in Fig. 9 for the $D \to pe$ and $D \to p\mu$ decay modes, respectively. In the absence of significant signals, ULs on the branching fractions in the range $(5-8) \times 10^{-7}$ at a 90% CL are obtained, depending on the decay mode.

4. Summary

The rare and symmetry violation charm decays are essential to probe new physics beyond the SM. Presents results are still above the SM predictions. And no obvious signals of new physics processes have been found yet. Fortunately, BESIII will have a 20 fb^{-1} data sample collected at 3.773 GeV [27], and LHCb will collect 50 fb^{-1} and 300 fb^{-1} data sample after upgrade [28], as well as the coming Belle II experiment. More and better results are coming soon.

References

[1] S. L. Glashow, J. Iliopoulos, and L. Maiani, Phys. Rev. D **2** 1285 (1970).

[2] G. Burdman, E. Golowich, J. A. Hewett, and S. Pakvasa, Phys. Rev. D **66**, 014009 (2002).

[3] I. I. Bigi and A. Paul, J. High Energy Phys. **03** 021 (2012).

[4] A. Paul, I. I. Bigi, and S. Recksiegel, Phys. Rev. D **83**, 114006 (2011).

[5] M. Ablikim *et al.* (BESIII Collaboration), Phys. Rev. D **105**, L071102 (2022).

[6] B. Holdom, Phys. Lett. B **166**, 196 (1986).

[7] B. A. Dobrescu, Phys. Rev. Lett. **94**, 151802 (2005).

[8] M. Ablikim *et al.* (BESIII Collaboration), Phys. Rev. D **106**, 072008 (2022).

[9] J. Y. Su and J. Tandean, Phys. Rev. D **102**, 115029 (2020).

[10] G. Burdman, E. Golowich, J. L. Hewett, and S. Pakvasa, Phys. Rev. D **66**, 014009 (2002).

[11] E. Golowich, J. A. Hewett, S. Pakvasa, and A. A. Petrov, Phys. Rev. D **79**, 114030 (2009).

[12] R. Aaij *et al.* (LHCb Collaboration), Phys. Rev. Lett. **131**, 041804 (2023).

[13] G. Buchalla, A.J. Buras, M.E. Lautenbacher, Rev. Mod. Phys. **68**, 1125 (1996).

[14] K.G. Wilson, Phys. Rev. **140**, B445 (1965).

[15] A. Khodjamirian, T. Mannel, A.A. Petrov, JHEP **11**, 142 (2015).

[16] B. Grinstein, J.M. Camalich, Phys. Rev. Lett. **116**, 141801 (2016).

[17] R. Aaij *et al.* (LHCb Collaboration), Eur. Phys. J. C **83**, 666 (2023).

[18] R. Aaij *et al.* (LHCb Collaboration), Phys. Rev. Lett. **128**, 221801 (2022).

[19] S. Fajfer, N. Kosnik, and S. Prelovsek Phys. Rev. D **76**, 074010 (2007).

[20] L. Cappiello, O. Cata, and G. D'Ambrosio, J. High Energy Phys. **04** (2013) 135.

[21] S. De Boer and G. Hiller, Phys. Rev. D **98**, 035041 (2018).

[22] F. Wilczek and A. Zee, Phys. Rev. Lett. **88**, 311 (1979).

[23] M. Ablikim *et al.* (BESIII Collaboration), Phys. Rev. D **105**, 032006 (2022).

[24] W. S. Hou, M. Nagashima, and A. Soddu, Phys. Rev. D **72**, 095001(2005).

[25] M. Ablikim *et al.* (BESIII Collaboration), Phys. Rev. D **106**, 112009(2022).

[26] S. Maity *et al.* (Belle Collaboration), Phys. Rev. D **109**, L031101 (2024).

[27] M. Ablikim *et al.* (BESIII Collaboration), Chin. Phys. C **44**, 040001 (2020).

[28] I. Bediaga *et al.* (LHCb Collaboration), arXiv:1808.08865